

Photovoltaic Hosting Capacity Sensitivity to Active Distribution Network Management

Mohammad Seydali Seyf Abad , Graduate Student Member, IEEE, and Jin Ma , Member, IEEE

Abstract—The increasing integration of rooftop photovoltaic (PV) systems in low voltage (LV) distribution systems may result in technical problems such as over-voltage. Thus, utilities have been employing different active distribution network management schemes to enhance rooftop photovoltaic hosting capacity (PVHC) by mitigating the technical issues. As there are different control schemes to resolve the over-voltage issue and increase PVHC, it is necessary to develop a comprehensive method to compare their effectiveness. The aim of this paper is to investigate the effects of autonomous voltage control strategies on the PVHC in LV distribution feeders. The investigated operation strategies are based on the active and reactive power control capabilities of PV systems as well as the on-load tap changer of transformers. We propose an optimization-based framework to determine the PVHC considering the voltage control capabilities. We do this by utilizing the linear mathematical model of the PVHC, in which the voltage control strategies are modeled as equality and inequality constraints. The proposed methodology is examined on IEEE 123-bus test system as well as 128 LV UK feeders to identify the potential of autonomous voltage control strategies in increasing the PVHC. Finally, the sensitivity of the obtained results to the R/X ratio of the feeders and size of PV systems is assessed.

Index Terms—Active power curtailment, distribution engineering, hosting capacity, on load tap changer, over-voltage, photovoltaic systems, reactive power control, secondary distribution systems.

NOMENCLATURE

ANM	Active Network Management.	$p_{i,t}^{g,\phi}$
APC	Active Power Curtailment.	\mathbf{PF}_i
$\mathbf{APC}_{i,t}$	The vector of active power curtailment at bus (i) and time (t).	\mathcal{P}^V
\mathbf{APCI}	Active Power Curtailment Indicator.	PV
$\mathbf{APCI}_i^{lpl}(t)$	Active power curtailment indicator for the (i^{th}) scenario of the LPL (lpl) at time (t).	PVHC
$\mathbf{APC}_{i,t}^\phi$	Curtailed active power at bus (i), phase (ϕ) and time (t).	$\mathbf{S}_{ij,t} = \mathbf{P}_{ij,t} + i\mathbf{Q}_{ij,t}$
\mathbf{Cap}_j^g	The vector of DERs installed capacity at bus (j) in different phases, which is defined as $[Cap_i^a, Cap_i^b, Cap_i^c]^T$.	$\mathbf{s}_{i,t}^d = \mathbf{p}_{i,t}^d + i\mathbf{q}_{i,t}^d$
		$\mathbf{p}_{i,t}^d = [p_{i,t}^{d,a}, p_{i,t}^{d,b}, p_{i,t}^{d,c}]^T$ and $\mathbf{q}_{i,t}^d = [q_{i,t}^{d,a}, q_{i,t}^{d,b}, q_{i,t}^{d,c}]^T$.
		The complex vector of three phase generated power at time (t), where, $\mathbf{p}_{i,t}^g = [p_{i,t}^{g,a}, p_{i,t}^{g,b}, p_{i,t}^{g,c}]^T$ and $\mathbf{q}_{i,t}^g = [q_{i,t}^{g,a}, q_{i,t}^{g,b}, q_{i,t}^{g,c}]^T$.
		SVR
		\mathcal{T}
		t_{ij}
		Step Voltage Regulator.
		Set of all time step over the study period.
		Tap of the transformer between bus (i) and (j).
		Constant Power Factor Mode.
		Distribution System Operator.
		Hosting Capacity.
		The total number of taps of the tap-changer of the transformer between bus (i) and (j).
		Set of all branches .
		Limitation of Active Power Feed-in Mode.
		Set of all location penetration levels.
		Location Penetration Level.
		Low Voltage.
		Vector of positive large numbers.
		Mixed Integer Linear Program.
		Minimum Photovoltaic Hosting Capacity.
		Medium Voltage.
		Set of buses.
		The number of pieces in the piecewise linear function.
		The length of binary representation of K_{ij} .
		Total number of expansion scenarios.
		On-Load Tap Changer.
		The maximum active power that can be curtailed at time (t).
		Active power that can be injected at bus (i), phase (ϕ) and time (t).
		The vector of power factor at bus (i).
		Set of buses that have PVs.
		Photovoltaic.
		Photovoltaic Hosting Capacity.
		The three phase complex power from bus (i) to bus (j) at time (t).
		The complex vector of three phase load at bus (i) and time (t), where

Manuscript received October 29, 2019; revised February 29, 2020, April 19, 2020, and May 30, 2020; accepted June 28, 2020. Date of publication July 8, 2020; date of current version January 6, 2021. Paper no. TPWRS-01639-2019. (Corresponding author: Mohammad Seydali Seyf Abad.)

The authors are with the School of Electrical and Information Engineering, The University of Sydney, Sydney, NSW 2006, Australia (e-mail: mohamad.seidaliseifabadi; j.ma@sydney.edu.au).

Color versions of one or more of the figures in this article are available online at <https://ieeexplore.ieee.org>.

Digital Object Identifier 10.1109/TPWRS.2020.3007997

Δt_{ij}	The turns ratio change per tap of the tap-changer of the transformer between bus (i) and (j).
t_{ij}^{\max}	The maximum turns ratio of the tap-changer of the transformer between bus (i) and (j).
t_{ij}^{\min}	The minimum turns ratio of the tap-changer of the transformer between bus (i) and (j).
TIC	Total Installed Capacity.
TIC_i^{lpl}	The total installed capacity for the (i^{th}) scenario of the LPL (lpl).
\mathbf{v}	The vector of upper voltage limit.
$\underline{\mathbf{v}}$	The vector of lower voltage limit.
\mathbf{v}_{band}	The acceptable error from the voltage reference.
$\mathbf{v}_{\text{far},t}$	The vector of three phase voltage of the farthest location from the transformer at time step (t).
$\mathbf{v}_{i,t}$	Define as $ \mathbf{V}_{i,t} = [V_{i,t}^a , V_{i,t}^b , V_{i,t}^c]^T$. Define as $[V_{i,t}^a ^2, V_{i,t}^b ^2, V_{i,t}^c ^2]^T$.
$\mathbf{v}_{i,t}^2$	The complex vector of three phase voltage at bus (i) and time (t).
$\mathbf{V}_{i,t}$	The nominal voltage in the system.
\mathbf{v}_{ref}	The voltage reference for the OLTC controller.
VVOM	Volt-Var Operation Mode.
VVWOM	Volt-Var-Watt Operation Mode.
VWOM	Volt-Watt Operation Mode.
$\mathbf{Z}_{ij} \in \mathbb{C}^{3 \times 3}$	The impedance complex matrix of branch (i, j).
$\eta_{j,t}^g$	The vector of capacity factor at bus (j) and time (t), which is defined as $[\eta_{j,t}^a, \eta_{j,t}^b, \eta_{j,t}^c]^T$.
θ	The rotation angle for counterclockwise rotation matrix.
$\lambda_{ij,\kappa}$	A binary variable.
$\Lambda_i^{lpl}(t)$	Total active power curtailment for the (i^{th}) scenario of the LPL (lpl) at time (t).
ρ	Maximum limitation on the feed-in active power.
Φ	Set of phases.
$\psi_{i,t,l}$	A vector of variables on interval $[0, 1]$.
$\omega_{i,t,l}$	A vector of binary variable.
\odot	Element-wise division.
\odot	Element-wise multiplication.

I. INTRODUCTION

IN THE last decade, integration of rooftop photovoltaic (PV) systems in low voltage (LV) distribution networks has increased significantly [1]. IEEE standard 241-1990 defined LV distribution systems as the systems with a voltage level below 600V [2]. High penetration of PV systems causes many technical issues in LV distribution systems. Hence, distribution system operators (DSOs) need to know the photovoltaic hosting capacity (PVHC), i.e. the maximum PV capacity that can be installed in the system irrespective of their locations without any network augmentation. Over-voltage is considered as one of the main

restriction for higher integration of PV systems [3]. This implies that DSOs can increase PVHC by addressing such an issue. The voltage regulation in distribution networks has been generally provided by on-load tap changer (OLTC) transformers that are installed in substations [4], step voltage regulators (SVR) [5] and reactive power compensation [6] along the feeders. In most of distribution networks, these voltage control devices are controlled based on local measurement, and are operated autonomously [7]. However, increasing penetration of distributed energy resources could have negative impact on the operation of non-coordinated OLTCs, SVRs, and voltage-controlled capacitor banks. For instance, increasing PV penetration level will yield in an increase in the number of OLTC and SVR operation, which will entail a higher maintenance cost for DSOs [8]. Besides classical grid augmentation measures, PV-based local control actions, as well as smart control of OLTC, which are also referred to as active distribution network management (ANM) schemes, can be used to alleviate the over-voltage problem [9]. So, it is important to understand and quantify the impact of ANM schemes on the PVHC.

Several methods for alleviating the voltage rise issue in presence of PV systems have been proposed. One simple method is decreasing the substation voltage using OLTC [10]. The effectiveness of this method highly depends on the control strategy and the location of the OLTC's control bus. Controlling the reactive power [11], [12], or curtailing the active power [13], [14] of PV systems by using local control actions are also utilized to address over-voltage issue. Another approach to resolve the over-voltage issue is controlling the active and reactive power of distributed energy resources using central controllers. This approach converges to the optimal solution as it is based on collecting all the available information into a central control unit and exploiting all of the available resources. Although, methods that are based on central controllers are generally more effective than those that are based on local controllers, the required infrastructure for implementing them is quite expensive. Though all these methods can be used for alleviating the voltage rise in distribution systems, their effectiveness in increasing the PVHC should be assessed and quantified. To do so, these ANM schemes should be considered in the PVHC estimation methodologies.

There are many methods for estimating the PVHC in distribution systems [15]–[20]. In [15]–[17], the location of PV systems are limited to a few specific locations, which results in over- or under-estimation of the PVHC. Some stochastic frameworks for estimating the PVHC, which are based on power flow simulations for a high number of PV expansion scenarios, are presented in [18]–[20]. Those frameworks, however, did not consider the control actions of PV systems and transformers' OLTC. Further, integrating local voltage control strategies in a power flow-based PVHC framework would be time-consuming, as identifying the power flow solution would require many iterations [21]–[23]. The study in [24] assessed the impact of feeder's properties on the effectiveness of local control actions. Nonetheless, the findings of that study were limited to a specific feeder.

A considerable part of the existing literature has focused on identifying the hosting capacity (HC) without considering the control schemes. Further, most of the studies that focused on increasing the HC using control schemes are hard to generalize as their findings are specific to their case study, albeit having real results. There are a few studies that attempted to assess the effectiveness of the control schemes in increasing the HC

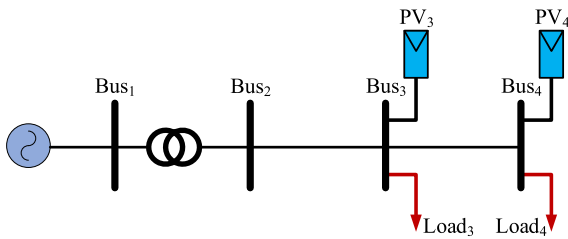


Fig. 1. Test system to illustrate the oscillation of local Volt-Var controllers.

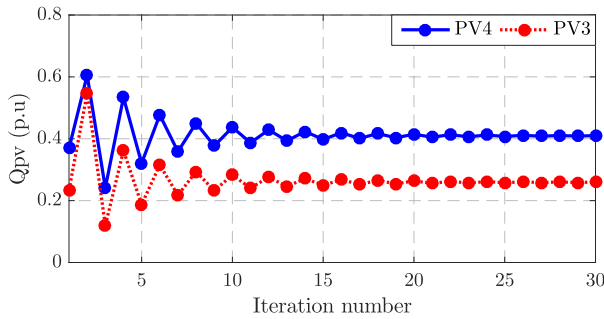


Fig. 2. The convergence of reactive power with Volt-Var controllers.

in multiple distribution systems [9], [20]. However, they either modeled distribution systems as balanced systems or focused on medium voltage (MV) distribution systems. Besides, the number of distribution systems assessed in those studies is limited, which means that they did not properly address the diversity and complexity of existing networks. Hence, it is difficult to generalize the findings of those studies.

Voltage control schemes in general and in particular local Volt-Var control schemes, are accompanied with several challenges including voltage oscillations [25], [26]. Therefore, integrating local Volt-Var controllers in power flow equations might result in an oscillatory behavior in the system. Convergence to the equilibrium point would be time-consuming as it requires running many power flow iterations. For instance, Fig. 1 shows a simple radial distribution system, where PV systems utilize the conventional Volt-Var droop control recommended by the IEEE 1547 standard [27]. As shown in Fig. 2, the reactive power of PV systems (Q_{PV}) oscillates and reaches an equilibrium point after 30 power flow iterations. To the best of the authors' knowledge, all existing studies that assessed the impacts of control schemes on the HC of a set of distribution systems integrated control schemes in power flow equations. Therefore, they would require numerous power flow iteration to identify the HC. Hence, they are computationally cumbersome. Thus, there is a need to develop a methodology to assess the effectiveness of control schemes in increasing the HC of distribution systems. Further, to address the diversity of the characteristics of LV networks, a high number of LV systems should be assessed.

In this paper, we assess the impacts of different voltage-related control schemes on the PVHC of distribution networks. It should be mentioned that the paper does not assume that the customer can directly control the voltage magnitude. However, it is assumed that the PV systems can exchange active/reactive powers based on local droop controllers. Although residential PV systems have been controlled at unity power factor, this

does not mean the Volt-Var and Volt-Watt controls will not become mandatory in future for small size PVs in secondary distribution level. For instance, from 2012, utilities in Germany are authorized to demand reactive power from distributed energy resources [10]. Further, a fixed limitation of active power feed-in is mandatory for newly installed small size PV systems that does not provide remote control capability to the utility [10]. This is just an indication that Volt-Var and Volt-Watt could be a potential option for improving the voltage profile in secondary distribution level. Though according to IEEE std 1547, Volt-Var and Volt-Watt capabilities are generally mandatory for distributed energy resources above 500 kVA, they could be a viable option for small size PV systems. Therefore, the aim of this paper is to investigate how much improvement these control strategies would entail if they also become mandatory for small size PV systems in future smart grids. The main contributions of this study are summarized as follows:

- 1) We propose an optimization-based framework to assess the impact of ANM schemes in increasing the PVHC. To do so, voltage control schemes including PV-based and OLTC-based control strategies are modeled as linear equality and inequality constraints in an optimization model. Further, unlike most of the studies, the network is modeled as an unbalanced system in the optimization problem. Moreover, a mathematical definition of minimum PVHC is laid out based on the solution of the developed optimization model. The main advantage of this method over the power flow method is that it converges to the solution without requiring more than one iteration.
- 2) To cover the diversity in the characteristics of distribution systems and draw some general conclusions, the proposed method is used to examine the effects of ANM schemes on increasing the PVHC on 128 LV UK feeders. Further, the total annual energy losses is defined as an index to assess the PV-based ANM schemes from an economic perspective.

The remainder of this paper is organized as follows: Section II describes the optimization-based framework to determine the PVHC. The problem formulation is presented in Section III. Section IV presents characteristics of the test feeders, as well as the numerical results and discussion. Finally, Section V summarizes the paper.

II. PROBABILISTIC FRAMEWORK

A stochastic framework as shown in Fig. 3 is developed to address the uncertainties in a practical approach. The framework includes three modules. The first module addresses the uncertainties associated with the number and location of PV systems by defining expansion scenarios. The second module addresses the uncertainties associated with the loads and output power of PV systems by solving the developed optimization model in Section III in a time series simulation. Then, the minimum PV hosting capacity (MPVHC) is identified based on the objective function values and active power curtailments (APCs) calculated in the second module. In the following, these three modules are explained in details.

Module 1) PV Expansion Scenarios: The number, location and size of PVs are three uncertain variables that depend on the customers' decision. A pragmatic approach to address these

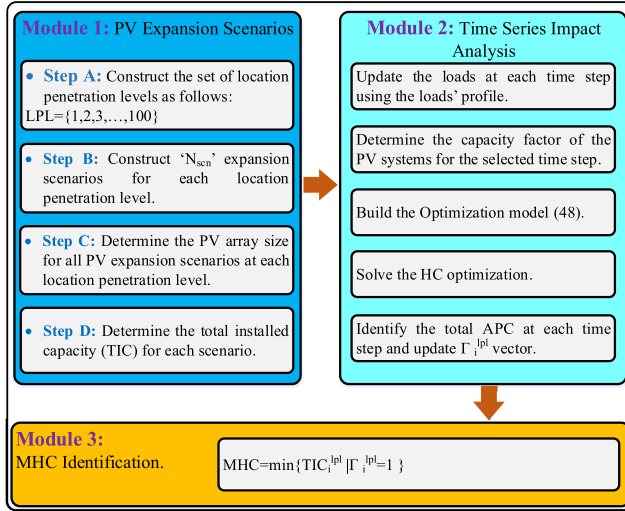


Fig. 3. The proposed PVHC analysis framework.

uncertainties is assessing the PVHC by generating a high number of scenarios. The steps for generating the scenarios are as follows:

- Step A:** This step addresses the uncertainty associated with the number of PV systems that could be installed. The minimum number of PV installation is zero and the maximum number is equal to the total number of customers. To cover a wide range of scenarios, the location penetration level (LPL), i.e. the ratio of the number of potential PV location to the total number of customers, is increased by a fixed step from 1% to 100%.
- Step B:** To address the uncertainty associated with the location of PV systems, a Monte Carlo approach is used to generate N_{scn} combinations of locations for each one of LPLs defined in Step A. Each combination is generated by random selection from the pool of all customers.
- Step C:** The base capacity of each of the combinations defined in Step B can be determined by sampling from the distribution function for the size of PV systems [28].
- Step D:** Considering the base capacity determined in Step C, the total installed capacity (TIC) for each scenario is calculated.

Module 2) Time Series Impact Analysis: This module addresses the uncertainties associated with the loads and output power of PV systems. The module is designed to assess whether the generated scenarios in Module 1 violates the operational constraints of the system over the study period or not. The core of this module is an optimization model, in which the operation criteria are modeled as equality and inequality constraints. Thus, the solution of this optimization model is used to identify the scenarios that violate the system constraints. The details of the optimization model are provided in Section III. The model is developed in a way that it converges in any condition. The total amount of APC is the indicator to detect the violation of the constraints over the study period. If the total amount of the APC is higher than the APC indicator (APCI), it implies that the scenario violates the operational constraints. The APCI for

different control strategies is as follows:

$$APCI_i^{lpl}(t) = \begin{cases} 0 & \text{No Control,} \\ 0 & \text{OLTC,} \\ 0 & \text{CPFM,} \\ \sum_{j \in \mathcal{N}} |(\eta_{j,t}^g - \rho) \odot \mathbf{Cap}_j|_1 & \text{LAPFM,} \\ 0 & \text{VVOM,} \\ \sum_{j \in \mathcal{N}} |\eta_{j,t}^g \odot \mathbf{Cap}_j|_1 & \text{VWOM,} \\ \sum_{j \in \mathcal{N}} |\eta_{j,t}^g \odot \mathbf{Cap}_j|_1 & \text{VVWOM,} \end{cases} \quad (1)$$

where, \odot denotes the element-wise multiplication; $APCI_i^{lpl}(t)$ is the APC indicator for the (i^{th}) scenario of the LPL (lpl) at time (t); OLTC, CPMF, LAPFM, VVOM, VWOM and VVWOM are different voltage control schemes that will be discussed in Section III; $\mathbf{Cap}_j = [Cap_j^a, Cap_j^b, Cap_j^c]^T$ represents the vector of PV inverter capacity; $\eta_{j,t}^g = [\eta_{j,t}^a, \eta_{j,t}^b, \eta_{j,t}^c]^T$ denotes the vector of capacity factors at bus (j) and at time (t); and ρ is the maximum limitation on the feed-in active power. By solving the developed optimization model (43) for the study period, i.e. all $t \in \mathcal{T}$, a vector Λ of length $|\mathcal{T}|$ is obtained for each expansion scenario. This vector contains the total APC for all $t \in \mathcal{T}$. A scenario violates the operational constraints if there is a time step in which the APC is higher than APCI. To mathematically represent this condition, for all $lpl \in \mathcal{LPL}$, the vector Γ^{lpl} is defined as follow:

$$\Gamma^{lpl}(j) = \begin{cases} 1 & \left(\sum_{t=1}^{|\mathcal{T}|} \Phi_j^{lpl}(t) \right) \geq 1 \\ 0 & \text{Otherwise} \end{cases} \quad j \in \{1 \dots N_{scn}\}, \quad (2)$$

where, \mathcal{LPL} is the set of all LPL and

$$\Phi_j^{lpl}(t) = \begin{cases} 1 & \Lambda(t)_j^{lpl} > APCI_j^{lpl}(t) \\ 0 & \text{Otherwise} \end{cases} \quad t \in \mathcal{T}. \quad (3)$$

Module 3) MPVHC Identification: Th MPVHC is defined as the lowest total PV capacity that yields a violation in the distribution system operational constraints. Based on this definition, the MPVHC can be mathematically formulated as follows:

$$MPVHC = \min_{lpl \in \mathcal{LPL}, 1 \leq i \leq N_{scn}} \{ TIC_i^{lpl} \mid \Gamma^{lpl}(i) = 1 \}, \quad (4)$$

where, TIC_i^{lpl} represents the TIC for the (i^{th}) scenario of the LPL (lpl).

III. PROBLEM FORMULATION

The PVHC is the minimum PV capacity that results in a violation of technical constraints in the system. The PVHC problem for a set of locations at time (t) can be formulated as an optimization problem as follows:

$$\text{minimize} \quad \sum_{i \in \mathcal{P}} \sum_{\phi \in \Phi} -p_{i,t}^{g,\phi} + APC_{i,t}^{\phi}, \quad (5)$$

where, \mathcal{P} is the set of buses that have PVs; Φ denotes the set of phases; $p_{i,t}^{g,\phi}$ denotes the active power that can be injected at bus (i), phase (ϕ) and time (t); and $APC_{i,t}^{\phi}$ represents the curtailed active power at bus (i), phase (ϕ) and time (t). The operation constraints are presented in Subsection III-A and III-B.

A. Distribution System Model

Consider a radial distribution network with N buses. Let $\mathcal{N} = \{1, \dots, N\}$ represent the set of all buses. Let \mathcal{L} denote the set of all branches, and (i, j) or $i \rightarrow j$ represent a branch between bus (i) and (j) in set \mathcal{L} . For every bus $i \in \mathcal{N}$, let $\mathbf{V}_{i,t} = [V_{i,t}^a, V_{i,t}^b, V_{i,t}^c]^T$ denote the complex vector of three phase voltage at time (t) , and $\mathbf{s}_{i,t}^d = \mathbf{p}_{i,t}^d + i\mathbf{q}_{i,t}^d$ represent the complex vector of three phase load at time (t) , where, $\mathbf{p}_{i,t}^d = [p_{i,t}^{d,a}, p_{i,t}^{d,b}, p_{i,t}^{d,c}]^T$ and $\mathbf{q}_{i,t}^d = [q_{i,t}^{d,a}, q_{i,t}^{d,b}, q_{i,t}^{d,c}]^T$. For every line $(i, j) \in \mathcal{L}$, $\mathbf{Z}_{ij} \in \mathbb{C}^{3 \times 3}$ denotes the impedance complex matrix, and $\mathbf{S}_{ij,t} = \mathbf{P}_{ij,t} + i\mathbf{Q}_{ij,t}$ represents the three phase complex power from bus (i) to bus (j) at time (t) . For every bus $i \in \mathcal{N}$, $\text{APC}_{i,t} = [\text{APC}_{i,t}^a, \text{APC}_{i,t}^b, \text{APC}_{i,t}^c]^T$ represents the vector of active power curtailment at time (t) , and $\mathbf{s}_{i,t}^g = \mathbf{p}_{i,t}^g + i\mathbf{q}_{i,t}^g$ denotes the complex vector of three phase generated power at time (t) , where, $\mathbf{p}_{i,t}^g = [p_{i,t}^{g,a}, p_{i,t}^{g,b}, p_{i,t}^{g,c}]^T$ and $\mathbf{q}_{i,t}^g = [q_{i,t}^{g,a}, q_{i,t}^{g,b}, q_{i,t}^{g,c}]^T$. Thus, the branch flow model can be summarized as follow:

$$\mathbf{v}_{j,t}^2 = \mathbf{v}_{i,t}^2 - 2(\tilde{\mathbf{r}}_{ij}\mathbf{P}_{ij,t} + \tilde{\mathbf{x}}_{ij}\mathbf{Q}_{ij,t}) + W_{ij}^v(\mathbf{P}_{ij,t}, \mathbf{Q}_{ij,t}), \quad (6)$$

where, $\mathbf{v}_{i,t} = |\mathbf{V}_{i,t}| = [|V_{i,t}^a|, |V_{i,t}^b|, |V_{i,t}^c|]^T$ and $\mathbf{v}_{i,t}^2 = [|V_{i,t}^a|^2, |V_{i,t}^b|^2, |V_{i,t}^c|^2]^T$.

$$\tilde{\mathbf{r}}_{ij} = \text{Re}\{\mathbf{a}_i \mathbf{a}_i^H\} \odot \text{Re}\{\mathbf{Z}_{ij}\} + \text{Im}\{\mathbf{a}_i \mathbf{a}_i^H\} \odot \text{Im}\{\mathbf{Z}_{ij}\}, \quad (7)$$

$$\tilde{\mathbf{x}}_{ij} = \text{Re}\{\mathbf{a}_i \mathbf{a}_i^H\} \odot \text{Im}\{\mathbf{Z}_{ij}\} - \text{Im}\{\mathbf{a}_i \mathbf{a}_i^H\} \odot \text{Re}\{\mathbf{Z}_{ij}\}, \quad (8)$$

$$\mathbf{a}_i = \left[1e^{-j2\pi/3} e^{j2\pi/3}\right]^T, \quad (9)$$

$$W_{ij}^v(\mathbf{P}_{ij}, \mathbf{Q}_{ij}) = [\mathbf{Z}_{ij} (\mathbf{S}_{ij} \ominus \mathbf{V}_i)^*] \odot [\mathbf{Z}_{ij}^* (\mathbf{S}_{ij} \ominus \mathbf{V}_i)]. \quad (10)$$

where, \odot and \ominus denote the element-wise multiplication and division, respectively. For every branch $(i, j) \in \mathcal{L}$, power balance equations are as follows:

$$\begin{aligned} \mathbf{P}_{ij,t} &= \sum_{k:j \rightarrow k} \mathbf{P}_{jk,t} + \mathbf{p}_{j,t}^d - \mathbf{p}_{j,t}^g + \text{APC}_{j,t} \\ &\quad + W_{ij}^p(\mathbf{P}_{ij,t}, \mathbf{Q}_{ij,t}), \end{aligned} \quad (11)$$

$$\mathbf{Q}_{ij,t} = \sum_{k:j \rightarrow k} \mathbf{Q}_{jk,t} + \mathbf{q}_{j,t}^d - \mathbf{q}_{j,t}^g + W_{ij}^q(\mathbf{P}_{ij,t}, \mathbf{Q}_{ij,t}), \quad (12)$$

$$\mathbf{p}_{j,t}^g \leq \eta_{j,t}^g \odot \mathbf{Cap}_j, \quad (13)$$

The terms $W_{ij}^v(\mathbf{P}_{ij,t}, \mathbf{Q}_{ij,t})$, $W_{ij}^p(\mathbf{P}_{ij,t}, \mathbf{Q}_{ij,t})$ and $W_{ij}^q(\mathbf{P}_{ij,t}, \mathbf{Q}_{ij,t})$ make equations (6), (11) and (12) nonlinear. To simplify the model, authors in [28] presented a method to linearize $W_{ij}^v(\mathbf{P}_{ij,t}, \mathbf{Q}_{ij,t})$, $W_{ij}^p(\mathbf{P}_{ij,t}, \mathbf{Q}_{ij,t})$, and $W_{ij}^q(\mathbf{P}_{ij,t}, \mathbf{Q}_{ij,t})$. Details on deriving these equations can be found in [28], [29]. Further, under normal operation of distribution networks, the following approximation is valid:

$$\mathbf{v}_{i,t}^2 - \mathbf{v}_{j,t}^2 \approx 2(\mathbf{v}_{i,t} - \mathbf{v}_{j,t}) \odot \mathbf{v}_{\text{nom}}, \quad (14)$$

where, \mathbf{v}_{nom} is the nominal voltage in the system. This approximation causes at most 0.25%–1% error when there is 5%–10%

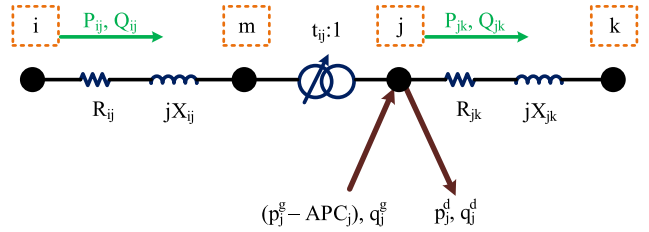


Fig. 4. The model of a transformer with on-load tap-changer (OLTC).

deviation in voltage magnitudes [30]. Thus, the linearized distribution system model can be established as follows:

$$\begin{aligned} \mathbf{v}_{j,t} &= \mathbf{v}_{i,t} - (\tilde{\mathbf{r}}_{ij}\mathbf{P}_{ij,t} + \tilde{\mathbf{x}}_{ij}\mathbf{Q}_{ij,t}) \odot \mathbf{v}_{\text{nom}} \\ &\quad + W_{ij}^v(\mathbf{P}_{ij,t}, \mathbf{Q}_{ij,t}) \odot (2\mathbf{v}_{\text{nom}}), \end{aligned} \quad (15)$$

$$\begin{aligned} \mathbf{P}_{ij,t} &= \sum_{k:j \rightarrow k} \mathbf{P}_{jk,t} + \mathbf{p}_{j,t}^d - \mathbf{p}_{j,t}^g + \text{APC}_{j,t} \\ &\quad + W_{ij}^p(\mathbf{P}_{ij,t}, \mathbf{Q}_{ij,t}), \end{aligned} \quad (16)$$

$$\mathbf{Q}_{ij,t} = \sum_{k:j \rightarrow k} \mathbf{Q}_{jk,t} + \mathbf{q}_{j,t}^d - \mathbf{q}_{j,t}^g + W_{ij}^q(\mathbf{P}_{ij,t}, \mathbf{Q}_{ij,t}), \quad (17)$$

where, $W_{ij}^v(\mathbf{P}_{ij,t}, \mathbf{Q}_{ij,t})$, $W_{ij}^p(\mathbf{P}_{ij,t}, \mathbf{Q}_{ij,t})$, and $W_{ij}^q(\mathbf{P}_{ij,t}, \mathbf{Q}_{ij,t})$ are the linear approximation of $W_{ij}^v(\mathbf{P}_{ij,t}, \mathbf{Q}_{ij,t})$, $W_{ij}^p(\mathbf{P}_{ij,t}, \mathbf{Q}_{ij,t})$, and $W_{ij}^q(\mathbf{P}_{ij,t}, \mathbf{Q}_{ij,t})$, respectively. Although using the linear model would entail 0.25%–1% error in the results, this level of error is justifiable as linearization would decrease the complexity of the model and make it easier to solve. Besides, even without linearization, there is some level of error in the estimated PVHC because of the uncertainties such as load variations, output power of PVs and PV locations. Further, it is possible to extract the probability distribution function (PDF) of the error between results of linear and nonlinear models. However, it is out of the scope of this study.

B. Modeling Active Distribution Network Management Schemes

There are different ANM schemes that can affect the PVHC of distribution systems. In the following, we presented the OLTC-based and PV-based ANM schemes as new constraints for the PVHC problem.

1) *OLTC Modeling*: Fig. 4 shows the model of a transformer that is installed between bus (i) and (j) . As it can be seen, the transformer is divided into two branches; branch (i, m) , which models the impedance of the transformer; and branch (m, j) , representing the tap-changer. The branch flow model for branch (i, m) is provided in equations (15)–(17). Further, the equation for tap-changer branch (m, j) is as follows:

$$\mathbf{v}_{m,t} = t_{ij}\mathbf{v}_{j,t}, \quad (18)$$

where, t_{ij} denotes the transformer tap, and

$$t_{ij} = t_{ij}^{\min} + T_{ij}\Delta t_{ij}, \quad 0 \leq T_{ij} \leq K_{ij}, \quad (19)$$

$$\Delta t_{ij} = (t_{ij}^{\max} - t_{ij}^{\min}) / K_{ij}, \quad (20)$$

where, t_{ij}^{\min} , t_{ij}^{\max} and K_{ij} represent the minimum turns ratio, the maximum turns ratio and the total taps of the tap-changer, respectively; Δt_{ij} denotes the turns ratio change per tap. Equation (18) has a nonlinear term. In order to represent it by linear equations, t_{ij} can be expressed by the binary expansion technique as follows [31]:

$$t_{ij} = t_{ij}^{\min} + \Delta t_{ij} \sum_{\kappa=0}^{N_{ij}} 2^\kappa \lambda_{ij,\kappa}, \quad (21)$$

$$\sum_{\kappa=0}^{N_{ij}} 2^\kappa \lambda_{ij,\kappa} \leq K_{ij}, \quad (22)$$

where, $\lambda_{ij,\kappa}$ is a binary variable; and N_{ij} is the length of binary representation of the total taps, i.e. K_{ij} . Multiplying both sides of equation (21) by $\mathbf{v}_{j,t}$ yields to:

$$\mathbf{v}_{m,t} = t_{ij}^{\min} \mathbf{v}_{j,t} + \Delta t_{ij} \sum_{\kappa=0}^{N_{ij}} 2^\kappa \mathbf{y}_{ij,\kappa}, \quad (23)$$

where, the variable $\mathbf{y}_{ij,\kappa} = \lambda_{ij,\kappa} \mathbf{v}_{j,t}$ can be replaced by the following equations:

$$0 \leq \mathbf{v}_{j,t} - \mathbf{y}_{ij,\kappa} \leq (1 - \lambda_{ij,\kappa}) \mathbf{M}, \quad (24)$$

$$0 \leq \mathbf{y}_{ij,\kappa} \leq \lambda_{ij,\kappa} \mathbf{M}, \quad (25)$$

where, \mathbf{M} is a vector of positive large numbers. Thus, instead of OLTC constraints (18)–(20), the mixed integer linear constraints (22)–(25) can be used. Finally, it should be noted that the OLTC can be controlled based on different schemes. The control schemes considered in this study are as follows:

- *OLTC-1*: OLTC controls the voltage of the secondary side of the transformer. This control schemes can be modeled as follows:

$$\mathbf{v}_{ref} - \frac{\mathbf{v}_{band}}{2} \leq \mathbf{v}_{j,t} \leq \mathbf{v}_{ref} + \frac{\mathbf{v}_{band}}{2}, \quad (26)$$

where, \mathbf{v}_{ref} is the voltage reference for the OLTC controller; and \mathbf{v}_{band} is the acceptable error from the voltage reference.

- *OLTC-2*: OLTC controls the voltage of the farthest location from the transformer. This control schemes can be modeled as follows:

$$\mathbf{v}_{ref} - \frac{\mathbf{v}_{band}}{2} \leq \mathbf{v}_{far,t} \leq \mathbf{v}_{ref} + \frac{\mathbf{v}_{band}}{2}, \quad (27)$$

where, $\mathbf{v}_{far,t}$ is the voltage of the farthest location from the transformer at time step (t).

- *OLTC-3*: OLTC attempts to keep the voltage of all buses in operation range. To implement this scheme, the following constraint should be added to the model.

$$\mathbf{v}_{i,t} \leq \bar{\mathbf{v}}, i \in \mathcal{N}, \quad (28)$$

where, $\bar{\mathbf{v}}$ is the vector of upper voltage limit.

2) *Inverter Modeling With Different Operation Mode*: An important factor that can affect the PVHC of a system is the control strategy that is used in PV systems. The area that the active and reactive power of PV systems on bus (i) could vary is represented as follows:

$$(\mathbf{p}_{i,t}^{\text{net}})^2 + (\mathbf{q}_{i,t}^g)^2 \leq (\mathbf{Cap}_i)^2, \quad (29)$$

where, $(\mathbf{q}_{i,t}^g)^2 = [(q_{i,t}^{g,a})^2, (q_{i,t}^{g,b})^2, (q_{i,t}^{g,c})^2]^T$ represents the element-wise square of the vector of generation reactive power at the bus (i) and time (t), $(\mathbf{Cap}_i)^2 = [(Cap_i^a)^2, (Cap_i^b)^2, (Cap_i^c)^2]^T$ denotes the element-wise square of the vector of inverter capacity at the bus (i), $(\mathbf{p}_{i,t}^{\text{net}})^2 = [(p_{i,t}^{\text{net},a})^2, (p_{i,t}^{\text{net},b})^2, (p_{i,t}^{\text{net},c})^2]^T$ and

$$\mathbf{p}_{i,t}^{\text{net}} = \mathbf{p}_{i,t}^g - \mathbf{APC}_{i,t}. \quad (30)$$

Equation (29) is a quadratic constraint. To linearize it, we rotate the tangent around the original circular constraint (29) using the counter clockwise rotation matrix as follows:

$$\mathbf{p}_{i,t}^{\text{net}} + \mathbf{q}_{i,t}^g \leq \sqrt{2} \mathbf{Cap}_i, \quad (31)$$

$$A = \begin{bmatrix} \cos(\theta) & -\sin(\theta) \\ \sin(\theta) & \cos(\theta) \end{bmatrix}, \quad (32)$$

where, θ is the rotation angle. Applying (32) to (31) results in:

$$[\cos(\theta) + \sin(\theta)] \mathbf{p}_{i,t}^{\text{net}} + [\cos(\theta) - \sin(\theta)] \mathbf{q}_{i,t}^g \leq \sqrt{2} \mathbf{Cap}_i. \quad (33)$$

The circular area presented by equation (29) constrains the active and reactive powers of a PV system based on the inverter capacity. Note that grid codes for PV systems usually add some other constraints, followings are some examples:

- 1) *Constant Power Factor Mode (CPFM)*: In this mode, the reactive power consumption of a PV system is proportional to its active power as follows:

$$\mathbf{q}_{i,t}^g = \tan(\arccos(\mathbf{PF}_i)) \mathbf{p}_{i,t}^{\text{net}}, \quad (34)$$

where, \mathbf{PF}_i is the vector of power factors at bus (i).

- 2) *Limitation of Active Power Feed-in Mode (LAPFM)*: Sometimes, a fixed limit on the feed-in active power of PV systems is mandatory. For instance, in Germany, the feed-in active power of PV systems that have a capacity of less than 30 kW and does not have the capability of being controlled remotely should always be below 70% of their installed capacity [10]. This constraint can be modeled as follows:

$$\mathbf{p}_{i,t}^{\text{net}} \leq \rho \mathbf{Cap}_i, \quad (35)$$

where, ρ is the maximum limitation on the feed-in active power.

- 3) *Volt-Var Operation Mode (VVOM)*: This mode is designed to actively limit the voltage rise at the PV connection point by controlling its reactive power based on the local voltage measurement. As it can be seen in Fig. 5, exceeding a certain voltage threshold activates the consumption of reactive power. The reactive power consumption is presented using a piecewise linear function as follows:

$$\mathbf{q}_{i,t}^g = f(\mathbf{v}_{i,t}) = \begin{cases} 0 & \mathbf{v}_0^q \leq \mathbf{v}_{i,t} \leq \mathbf{v}_1^q, \\ \alpha_{i,t} \frac{\mathbf{v}_{i,t} - \mathbf{v}_1^q}{\mathbf{v}_{\text{nom}}} \mathbf{q}_{i,t}^{\max} & \mathbf{v}_1^q \leq \mathbf{v}_{i,t} \leq \mathbf{v}_2^q, \\ -\mathbf{q}_{i,t}^{\max} & \mathbf{v}_2^q \leq \mathbf{v}_{i,t} \leq \mathbf{v}_3^q, \end{cases} \quad (36)$$

where, $\mathbf{q}_{i,t}^{\max}$ is the maximum available reactive power capacity at time (t); and

$$\mathbf{q}_{i,t} = \mathbf{v}_{\text{nom}} \ominus (\mathbf{v}_1^q - \mathbf{v}_2^q). \quad (37)$$

Note that the above piecewise linear functions are nonlinear over the defined range, as shown in Fig. 5. It is possible

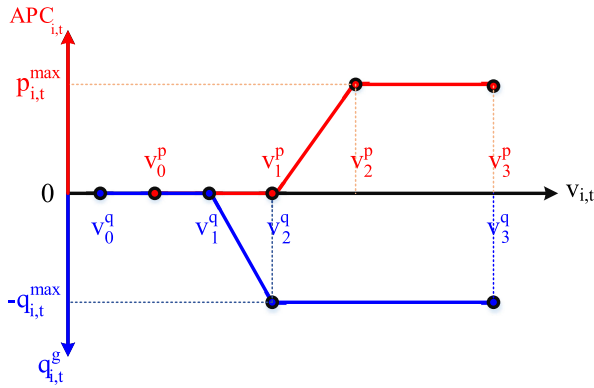


Fig. 5. The VWOM and VVOM local control schemes.

to represent $q_{i,t}^g$ as a set of linear constraints by defining a set of new variables as follows:

$$q_{i,t}^g = \sum_{l=0}^{N_{BC}} \psi_{i,t,l} \odot f(v_l^q), \quad (38a)$$

$$0 \leq \psi_{i,t,0} \leq \omega_{i,t,0}, \quad (38b)$$

$$0 \leq \psi_{i,t,l} \leq \omega_{i,t,l-1} + \omega_{i,t,l}, l = 1, \dots, N_{BC} - 1, \quad (38c)$$

$$0 \leq \psi_{i,t,N_{BC}} \leq \omega_{i,t,N_{BC}-1}, \quad (38d)$$

$$\sum_{l=0}^{N_{BC}-1} \omega_{i,t,l} = 1, \quad (38e)$$

$$\sum_{l=0}^{N_{BC}} \psi_{i,t,l} = 1, \quad (38f)$$

$$v_{i,t} = \sum_{l=0}^{N_{BC}} \psi_{i,t,l} \odot v_l^q, \quad (38g)$$

$$\psi_{i,t,l} \geq 0, l = 1, \dots, N_{BC}, \quad (38h)$$

$$\omega_{i,t,l} \in \{0, 1\}, l = 0, \dots, N_{BC} - 1, \quad (38i)$$

where, N_{BC} is the number of pieces in the piecewise linear function; $\omega_{i,t,l}$ and $\psi_{i,t,l}$ are the vector of binary and continuous variables, respectively. Thus, linear constraints (38a)-(38i) can replace nonlinear constraint (36).

- 4) *Volt-Watt Operation Mode (VWOM)*: This mode is designed to actively limit the voltage rise at the PV connection point by curtailing the PV active power based on the local voltage measurement. As shown in Fig. 5, exceeding a certain voltage threshold activate the active power curtailment. Similar to the VVOM, active power curtailment can be modeled as follows:

$$APC_{i,t} = \begin{cases} 0 & v_0^p \leq v_{i,t} \leq v_1^p, \\ \beta_{i,t} \frac{v_{i,t} - v_1^p}{v_{nom}} p_{i,t}^{max} & v_1^p \leq v_{i,t} \leq v_2^p, \\ p_{i,t}^{max} & v_2^p \leq v_{i,t} \leq v_3^p, \end{cases} \quad (39)$$

$$APC_{i,t} \leq p_{i,t}^g, \quad (40)$$

where, $p_{i,t}^{max}$ is the maximum active power that can be curtailed at time (t) and

$$\beta_{i,t} = v_{nom} \ominus (v_2^p - v_1^p). \quad (41)$$

Further, the linearization technique for (36) can be used to linearize the piecewise constraint (39) as well.

- 5) *Volt-Var-Watt Operation Mode (VVWOM)*: This mode is the combination of VVOM and VWOM, as shown in Fig. 5.

C. Other Technical Constraints

Over-voltage is the most important technical constraint, which is presented as follows:

$$\underline{v} \leq v_{i,t} \leq \bar{v}. \quad (42)$$

Altogether, considering the ANM schemes, the PVHC at time (t) can be modeled as a Mixed Integer Linear Program (MILP) as follows:

$$\begin{aligned} & \text{minimize} \quad \sum_{i \in \mathcal{PV}} \sum_{\phi \in \Phi} -p_{i,t}^{g,\phi} + APC_{i,t}^\phi, \\ & \text{s.t.} \\ & (15)-(17), (22)-(28) \\ & (33), (34), (35), (37), (38), \\ & \text{Linear equivalent of (39), (40)-(42).} \end{aligned} \quad (43)$$

The CPLEX solver has been used to solve the optimization model.

IV. EVALUATION AND ASSESSMENT

In this section, simulations are carried out to assess the performance of the proposed methodology. Initially, the performance of the developed method is examined on IEEE 123-bus system. Then, the efficacy of the proposed framework in evaluation of 128 LV UK feeders is shown. Finally, the sensitivity of the results to the PV size is assessed using the proposed framework.

A. Test Systems

The developed method is applied to IEEE 123-bus system [32] as well as 128 LV UK feeders [19]. Some important characteristics of UK feeders are presented in Fig. 6. The topology of 7 UK feeders is presented in Fig. 7. The rated power of the service transformers in UK feeders is 800 kVA, and the voltages in primary and secondary circuits are 11 kV and 0.415 kV, respectively. The load profiles are created using the tool presented in [33]. The normalized PV profiles are derived from the tool presented in [34]. As for the size of PV systems, a base capacity of 100 kW is considered for PV systems in IEEE 123-bus system. Further, 37% of the installed PV systems in the UK is 4 kW, which is the most common PV size in the UK [19]. Thus, a base capacity of 4 kW is considered for PV systems in UK feeders. The maximum acceptable voltage is 1.05 p.u.

B. Performance Assessment in IEEE 123-Bus System

The performance of the proposed method is examined using IEEE 123-bus system. The results of the proposed method is compared with those of power flow-based Monte Carlo approach presented in [9]. The main idea of the approach presented in [9]

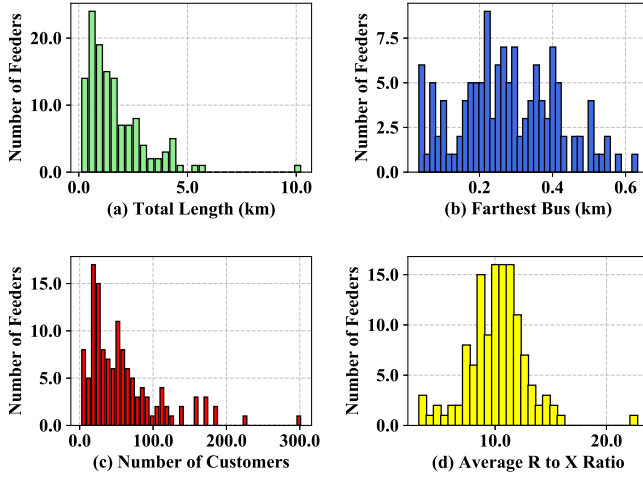


Fig. 6. Some of the key characteristics of 128 LV UK feeders including: (a) the distribution of total length of the feeders; (b) the distribution of farthest node from the service transformer; (c) the distribution of number of customers; (d) the distribution of average R to X ratio.

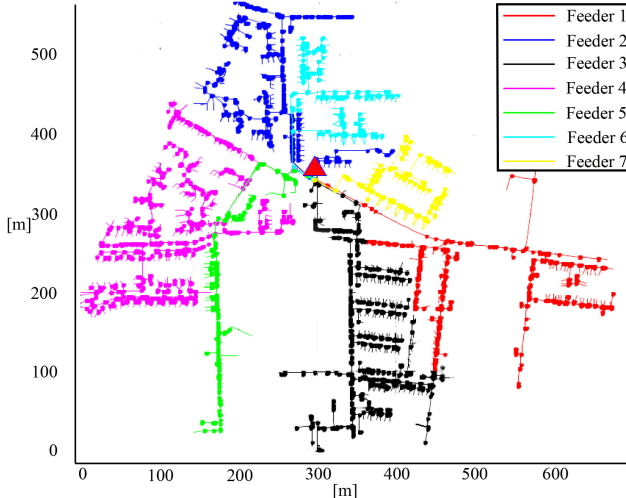


Fig. 7. Topology of 7 LV UK feeders.

is increasing the penetration level of PV systems and performing the power flow calculation in MATPOWER [35]. Further, a worst-case assumption is made, which is simulating the low load with high generation condition. In order to increase the accuracy of the presented approach in [9], the procedure is repeated 200 times. Fig. 8 demonstrates the MPVHC in IEEE 123-bus system for the proposed and Monte Carlo approaches. As can be seen, both methods show a similar trend in effectiveness of PV-based control strategies. For instance, both methods showed that VVOM is more effective than LAPFM and CPFM in increasing MPVHC. However, there is some differences in performance of the proposed method and the Monte Carlo approach. Observe that the estimated MPVHC for the test network without any PV-based control strategy by the proposed method is 13.187%, which is 3.297% higher than that of the Monte Carlo approach. Further, the estimated MPVHC by the proposed method for VVOM is 10.989% higher than that of the Monte Carlo approach. This is mainly because of the worst-case assumption that

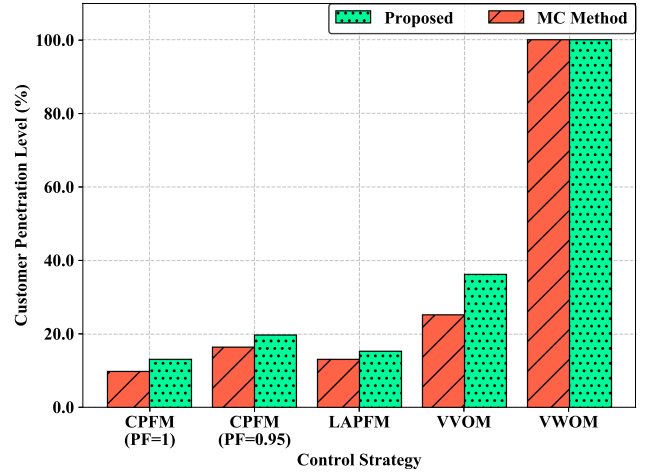


Fig. 8. MPVHC in IEEE 123-bus system using the proposed and Monte Carlo methods for different PV-based control schemes.

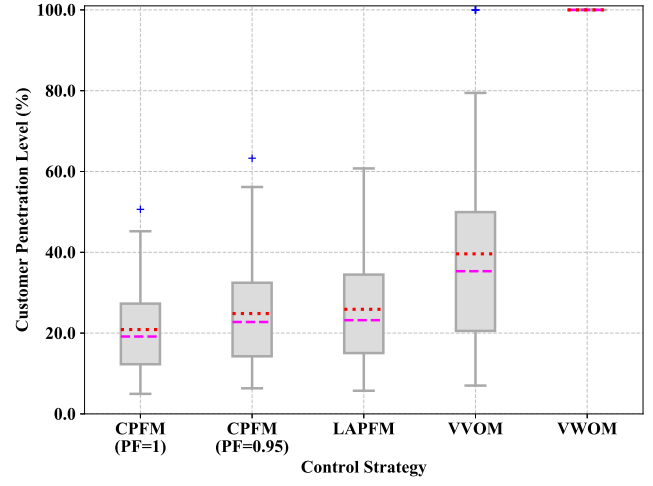


Fig. 9. The effect of PV-based ANM including CPFM, LAPFM, VVOM and VWOM on the MPVHC of studied feeders.

has been made in the considered Monte Carlo approach. Thus, the worst-case assumption can cause underestimation of control strategies' effectiveness in increasing the MPVHC. Further, as it was shown, the proposed method provides a more accurate result than the Monte Carlo approach.

C. Performance Assessment in 128 UK Feeders

To clarify the sensitivity of the MPVHC, it is necessary to identify the MPVHC of the systems without exploiting the ANM schemes. The simulation results showed that 72 feeders do not have PVHC issue, i.e., if every customer in these feeders installs a 4 kW PV system, there will be no voltage violation in the system. However, 56 feeders are limited by voltage constraint and have a PVHC of less than 55%. This indicates that almost half of the studied feeders will experience voltage violation issues with a high penetration of PV systems.

Fig. 9 shows the box plot of the MPVHC for different PV-based ANM schemes. On each box, the red dots and purple dash marks are the mean and median, the horizontal edges are

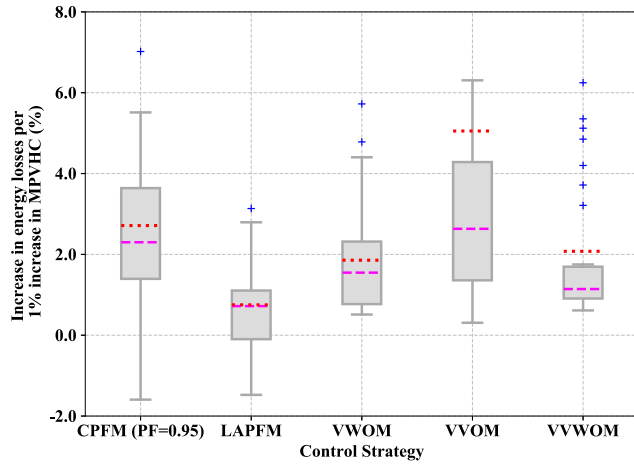


Fig. 10. The averaged increase in the total annual energy losses including the PV systems' curtailed energy and the feeders' energy loss due to 1% increase in the MPVHC using PV-based ANM schemes.

the 25th and 75th percentiles, the whiskers extend to the most extreme values not considered outliers, and outliers are plotted individually. Observe that operation of the PV systems at a constant power factor of 0.95 lag only increased the MPVHC with an average of 3.96%. Further, limiting the output power of the PV systems to 70% of their installed capacity increased the MPVHC on average by 5.013%. Whereas, VVOM increased the MPVHC on average by 18.74%, which is much higher than the MPVHC change due to operation of PVs in CPFM and LAPFM operation modes. It can also be seen in Fig. 9 that the most effective PV-based operation mode is VWOM. Observe that using VWOM increased the MPVHC to 100% in all the studied feeders. VWOM, however, is not an interesting operation strategy from the customers' point of view as they pay the costs of increasing the MPVHC. Thus, if the customers have to be involved in improving the network, VVOM could be a more attractive option from the customers' standpoint. VVOM, however, can increase the costs of DSOs by increasing the power losses in the system. Fig. 10 depicts the average increase in the total annual energy losses including the PV systems' curtailed energy and the feeders' energy loss due to 1% increase in the MPVHC using PV-based ANM schemes. Observe that CPFM and VVOM, which are reactive power-based ANM schemes, increased the total annual energy losses on average by 2.73% and 5.05% per 1% increase in the MPVHC, respectively. The average change in total annual energy losses per 1% increase in the MPVHC for these two control strategies is higher than that of other schemes. Hence, although reactive power-based control schemes seem more attractive, they cost more than other schemes to increase the MPVHC. Further, LAPFM caused an average increase of 0.75%, which is the lowest among all the control strategies. VWOM with an average increase of 1.86% is the second lowest among all the control schemes. Considering that the LAPFM scheme has much less capability than VWOM to increase the MPVHC, it can be concluded that VWOM is a better scheme for increasing the MPVHC.

Another set of ANM schemes are based on OLTC. Generally, it is believed that OLTC can increase the MPVHC of a system. However, it is the control strategy that determines the effectiveness of OLTC. Fig. 11 depicts the box plot of MPVHC for **OLTC-1**, **OLTC-2** and **OLTC-3** with reference to CPFM with

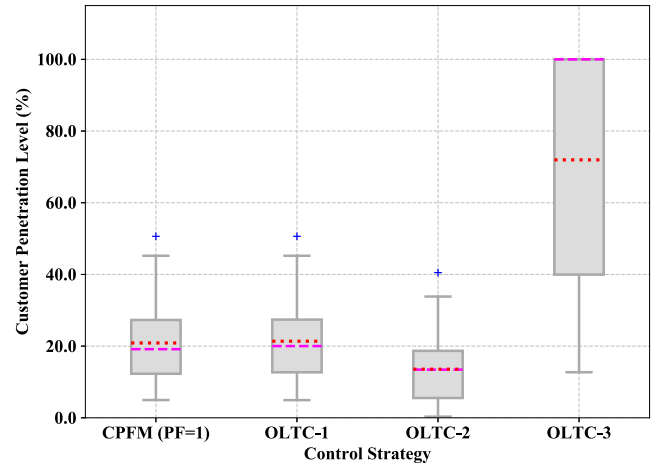


Fig. 11. The effect of OLTC-based ANM on the MPVHC of studied feeders.

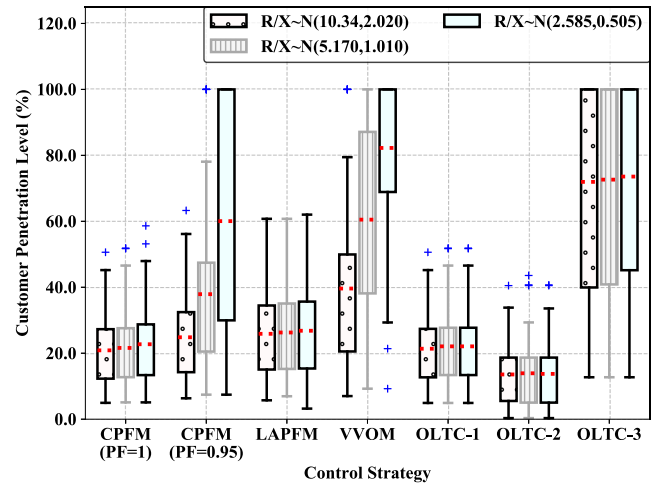


Fig. 12. The impact of R/X ratio on the effectiveness of autonomous voltage control strategies in increasing the MPVHC.

unity power factor. It can be seen that when the OLTC controlled the voltage of transformer secondary winding (**OLTC-1**), it only increased the MPVHC on average by 0.49%. However, when the OLTC controller operated based on the feedback from all buses of the system (**OLTC-3**), it increased the MPVHC on average by 51.08%. Although **OLTC-3** would increase MPVHC effectively, it requires an extensive communications infrastructure. Interestingly, when the OLTC controlled the voltage of the farthest bus from the transformer (**OLTC-2**), it decreased the MPVHC on average by 7.30%.

An important parameter that can impact the effectiveness of voltage control schemes is R/X ratio. In this study, the R/X ratio of a feeder is defined as the weighted arithmetic mean of R/X ratio of its lines. As it can be seen in Fig. 6(d), the R/X ratio of the investigated systems has a Gaussian distribution with an average of 10.34 and standard deviation of 2.02. A sensitivity analysis is performed to evaluate the impact of R/X on the effectiveness of the autonomous voltage control strategies in increasing the MPVHC. To do so, the R/X ratio of all the investigated systems are changed to half and a quarter of the original values and the PHVC framework is run again. Fig. 12 shows the impact

of R/X ratio on the effectiveness of voltage control strategies. As it can be seen, the effectiveness of Volt-Var operation mode in increasing the MPVHC increases by decreasing the R/X ratio, which implies that in systems with low R/X ratio, the reactive power-based schemes are really effective for increasing the MPVHC. Nevertheless, as it was shown in Fig. 10, these schemes are more costly than others. Further, it was observed that increasing X/R ratio did not have a tangible effect on the performance of OLTC- and APC-based schemes. The simulation results are consistent with the general belief that reactive power control strategies are more effective when R/X ratio is low. Moreover, it is generally believed that APC can be more effective than reactive power control in the networks with a high R/X ratio. However, this does not mean that any APC-based scheme could be more effective than reactive power-based schemes. As shown in Fig. 12, VVOM, which is based on exchanging reactive power is more effective than LAPFM, which is based on APC. Therefore, R/X ratio can not be the only index to judge the effectiveness of different control schemes.

In this paper, the effectiveness of a range of voltage control schemes in increasing MPVHC has been discussed. However, it is also important to discuss the findings of this study from a practical perspective. As it was shown in Fig. 11, OLTC could effectively increase MPVHC. Nevertheless, OLTC is usually used in MV systems. Although utilizing OLTCs for voltage management in LV systems has been recently studied, they have not been used very often in real LV systems. Thus, considering the additional cost for installing a transformer with OLTC in LV systems, it is necessary to perform a cost-benefit assessment. Moreover, the costs of network reinforcement measures such as changing transformer and installing additional cables would make the PV-based control schemes a more attractive option to increase MPVHC.

D. Sensitivity to the PV Size

In Section IV-C, it is assumed that the base capacity of PV systems is 4 kW. However, in this section, it is assumed that the size of PV systems follows an empirical distribution. According to the historical statistics of UK, the probability of installing a PV system with a size of 1, 1.5, 2, 2.5, 3, 3.5, and 4 kW is 1%, 8%, 13%, 14%, 14%, 12% and 37%, respectively [19]. The proposed method is applied to 128 LV UK feeders. Fig. 13 demonstrates the MPVHC for different PV-based ANM schemes.

It can be observed that the MPVHC is higher when the size of PV systems is selected based on the empirical distribution in comparison to when the base PV size is set at 4 kW. However, in terms of the effectiveness of control schemes to increase the MPVHC, the trend is the same as when the PV size is set at 4 kW. Observe that when the size of PV systems is selected based on the empirical distribution, controlling the PV systems at a constant power factor of 0.95 lag only increased the MPVHC with an average of 5.85%. Further, limiting the output power of the PV systems to 70% of their installed capacity increased the MPVHC on average by 7.19%. Moreover, VVOM increased the MPVHC on average by 20.94%, which is much higher than the MPVHC change due to operation of PVs in CPFPM and LAPFM operation modes. Note that sampling from empirical distribution of PV systems mainly increased the MPVHC. However, it would not majorly impact the effectiveness of control schemes in increasing the MPVHC.

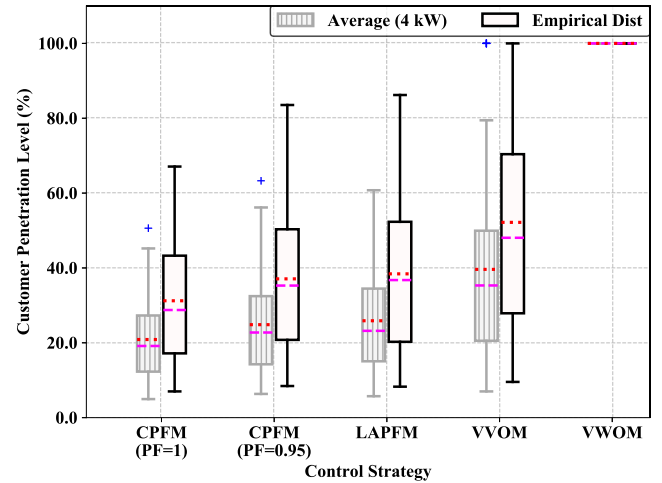


Fig. 13. The impact of size of PV systems on the effectiveness of different control schemes.

V. CONCLUSION

In this paper, the impact of different autonomous voltage control strategies for increasing the PVHC in radial distribution systems were studied. The investigated schemes included PV-based local control actions, as well as controlling the OLTC of the transformer. In order to integrate these voltage control schemes into the PVHC studies, a modular optimization-based framework was proposed. The proposed method is examined on 128 LV UK feeders. Following are the conclusions derived from the simulation results:

- Active power curtailment mode, i.e. VWOM, is the most effective control scheme to increase MPHVC. This control scheme increases MPVHC to 100% in any distribution feeder. Further, simulation result showed that Volt-Var operation mode of PV systems, i.e. VVOM, is the second most effective PV-based control scheme with an average increase of 18.74% in MPVHC.
- Active power based control strategies, i.e. LAPFM and VWOM, resulted in the lowest total energy losses per 1% increase in MPVHC among all PV-based control schemes. This means that in the feeders with R/X ratio higher than 5, the active power based control schemes are more cost effective than reactive power based control schemes to increase MPVHC.
- The impact of OLTC on MPVHC highly depends on its control strategy. It was shown that if the aim of OLTC controller is controlling the voltage at the end of a feeder, it decreases the MPVHC. Nevertheless, if the aim is to maintain the voltage of all the locations in the feeder within permissible bounds, it can increase the MPVHC on average by 51.08%.
- The performance of reactive power based schemes highly depends on the R/X ratio. For instance, the simulation result showed that VVOM control scheme increased MPVHC on average by 18.74% in a set of feeders with an average R/X ratio of 10.34. Nevertheless, VVOM scheme increased MPVHC on average by 38.9% in a set of feeders with an average R/X ratio of 5.17. Finally, it was shown that X/R ratio does not have a tangible impact on the performance of OLTC- and APC-based schemes.

REFERENCES

- [1] B. Bayer, P. Matschoss, H. Thomas, and A. Marian, "The German experience with integrating photovoltaic systems into the low-voltage grids," *Renewable Energy*, vol. 119, pp. 129–141, 2018.
- [2] *IEEE Recommended Practice for Electric Power Systems in Commercial Buildings*, IEEE Standard 241-1990, pp. 1–768, Sep. 1991.
- [3] X. Chen, W. Wu, and B. Zhang, "Robust capacity assessment of distributed generation in unbalanced distribution networks incorporating ANM techniques," *IEEE Trans. Sustain. Energy*, vol. 9, no. 2, pp. 651–663, Apr. 2018.
- [4] S. N. Salih and P. Chen, "On coordinated control of OLTC and reactive power compensation for voltage regulation in distribution systems with wind power," *IEEE Trans. Power Syst.*, vol. 31, no. 5, pp. 4026–4035, Sep. 2016.
- [5] D. Ranamuka, A. P. Agalgaonkar, and K. M. Muttaqi, "Online voltage control in distribution systems with multiple voltage regulating devices," *IEEE Trans. Sustain. Energy*, vol. 5, no. 2, pp. 617–628, Apr. 2014.
- [6] N. Daratha, B. Das, and J. Sharma, "Coordination between OLTC and SVC for voltage regulation in unbalanced distribution system distributed generation," *IEEE Trans. Power Syst.*, vol. 29, no. 1, pp. 289–299, Jan. 2014.
- [7] Y. P. Agalgaonkar, B. C. Pal, and R. A. Jabr, "Distribution voltage control considering the impact of PV generation on tap changers and autonomous regulators," *IEEE Trans. Power Syst.*, vol. 29, no. 1, pp. 182–192, Jan. 2014.
- [8] F. Katiraei and J. R. Aguero, "Solar PV integration challenges," *IEEE Power Energy Mag.*, vol. 9, no. 3, pp. 62–71, May 2011.
- [9] T. Stetz, K. Diwold, M. Kraiczy, D. Geibel, S. Schmidt, and M. Braun, "Techno-economic assessment of voltage control strategies in low voltage grids," *IEEE Trans. Smart Grid*, vol. 5, no. 4, pp. 2125–2132, Jul. 2014.
- [10] T. Stetz, F. Marten, and M. Braun, "Improved low voltage grid-integration of photovoltaic systems in Germany," *IEEE Trans. Sustain. Energy*, vol. 4, no. 2, pp. 534–542, Apr. 2013.
- [11] E. Demirok, P. C. Gonzalez, K. H. B. Frederiksen, D. Sera, P. Rodriguez, and R. Teodorescu, "Local reactive power control methods for overvoltage prevention of distributed solar inverters in low-voltage grids," *IEEE J. Photovolt.*, vol. 1, no. 2, pp. 174–182, Oct. 2011.
- [12] A. Safayet, P. Fajri, and I. Husain, "Reactive power management for overvoltage prevention at high PV penetration in a low-voltage distribution system," *IEEE Trans. Ind Appl.*, vol. 53, no. 6, pp. 5786–5794, Nov. 2017.
- [13] R. Tonkoski, L. A. C. Lopes, and T. H. M. El-Fouly, "Coordinated active power curtailment of grid connected PV inverters for overvoltage prevention," *IEEE Trans. Sustain. Energy*, vol. 2, no. 2, pp. 139–147, Apr. 2011.
- [14] D. V. Bozalakov, T. L. Vandoorn, B. Meersman, G. K. Papagiannis, A. I. Chrysochos, and L. Vandeveldt, "Damping-based droop control strategy allowing an increased penetration of renewable energy resources in low-voltage grids," *IEEE Trans. Power Del.*, vol. 31, no. 4, pp. 1447–1455, Aug. 2016.
- [15] A. Hoke, R. Butler, J. Hambrick, and B. Kroposki, "Steady-state analysis of maximum photovoltaic penetration levels on typical distribution feeders," *IEEE Trans. Sustain. Energy*, vol. 4, no. 2, pp. 350–357, Apr. 2013.
- [16] R. A. Shayani and M. A. G. de Oliveira, "Photovoltaic generation penetration limits in radial distribution systems," *IEEE Trans. Power Syst.*, vol. 26, no. 3, pp. 1625–1631, Aug. 2011.
- [17] X. Chen, W. Wu, B. Zhang, and C. Lin, "Data-driven DG capacity assessment method for active distribution networks," *IEEE Trans. Power Syst.*, vol. 32, no. 5, pp. 3946–3957, Sep. 2017.
- [18] A. Dubey and S. Santoso, "On estimation and sensitivity analysis of distribution circuit's photovoltaic hosting capacity," *IEEE Trans. Power Syst.*, vol. 32, no. 4, pp. 2779–2789, Jul. 2017.
- [19] A. Navarro-Espinosa and L. F. Ochoa, "Probabilistic impact assessment of low carbon technologies in LV distribution systems," *IEEE Trans. Power Syst.*, vol. 31, no. 3, pp. 2192–2203, May 2016.
- [20] F. Ding and B. Mather, "On distributed PV hosting capacity estimation, sensitivity study, and improvement," *IEEE Trans. Sustain. Energy*, vol. 8, no. 3, pp. 1010–1020, Jul. 2017.
- [21] K. Baker, A. Bernstein, E. Dall'Anese, and C. Zhao, "Network-cognizant voltage droop control for distribution grids," *IEEE Trans. Power Syst.*, vol. 33, no. 2, pp. 2098–2108, Mar. 2018.
- [22] M. Farivar, X. Zho, and L. Che, "Local voltage control in distribution systems: An incremental control algorithm," in *Proc. IEEE Int. Conf. Smart Grid Commun.*, Nov. 2015, pp. 732–737.
- [23] X. Zhou, J. Tian, L. Chen, and E. Dall'Anese, "Local voltage control in distribution networks: A game-theoretic perspective," in *Proc. North Amer. Power Symp.*, Sep. 2016, pp. 1–6.
- [24] B. Bleitterie, S. Kadam, R. Bolgaryn, and A. Zegers, "Voltage control with PV inverters in low voltage networks-in depth analysis of different concepts and parameterization criteria," *IEEE Trans. Power Syst.*, vol. 32, no. 1, pp. 177–185, Jan. 2017.
- [25] H. Sun *et al.*, "Review of challenges and research opportunities for voltage control in smart grids," *IEEE Trans. Power Syst.*, vol. 34, no. 4, pp. 2790–2801, Jul. 2019.
- [26] A. Singhal, V. Ajjarapu, J. C. Fuller, and J. Hansen, "Real-time local volt/var control under external disturbances with high PV penetration," *IEEE Trans. Smart Grid*, vol. 10, no. 4, pp. 3849–3859, Jul. 2019.
- [27] *IEEE Standard for Interconnection and Interoperability of Distributed Energy Resources With Associated Electric Power Systems Interfaces*, IEEE Standard 1547-2018 (Revision of IEEE Standard 1547-2003), pp. 1–138, Apr. 2018.
- [28] M. S. S. Abad, J. Ma, D. Zhang, A. S. Ahmadyar, and H. Marzooghi, "Probabilistic assessment of hosting capacity in radial distribution systems," *IEEE Trans. Sustain. Energy*, vol. 9, no. 4, pp. 1935–1947, Oct. 2018.
- [29] B. A. Robbins and A. D. Dominguez-Garcia, "Optimal reactive power dispatch for voltage regulation in unbalanced distribution systems," *IEEE Trans. Power Syst.*, vol. 31, no. 4, pp. 2903–2913, Jul. 2016.
- [30] H. Zhu and H. J. Liu, "Fast local voltage control under limited reactive power: Optimality and stability analysis," *IEEE Trans. Power Syst.*, vol. 31, no. 5, pp. 3794–3803, Sep. 2016.
- [31] W. Wu, Z. Tian, and B. Zhang, "An exact linearization method for OLTC of transformer in branch flow model," *IEEE Trans. Power Syst.*, vol. 32, no. 3, pp. 2475–2476, May 2017.
- [32] W. H. Kersting, "Radial distribution test feeders," *IEEE Trans. Power Syst.*, vol. 6, no. 3, pp. 975–985, Aug. 1991.
- [33] I. Richardson, M. Thomson, D. Infield, and C. Clifford, "Domestic electricity use: A high-resolution energy demand model," *Energy Buildings*, vol. 42, no. 10, pp. 1878–1887, 2010.
- [34] S. Pfenninger and I. Staffell, "Long-term patterns of European PV output using 30 years of validated hourly reanalysis and satellite data," *Energy*, vol. 114, pp. 1251–1265, 2016.
- [35] R. D. Zimmerman, C. E. Murillo-Sánchez, and R. J. Thomas, "MATPOWER: Steady-state operations, planning, and analysis tools for power systems research and education," *IEEE Trans. Power Syst.*, vol. 26, no. 1, pp. 12–19, Feb. 2011.